μ approach to robust stability domains in the space of parametric uncertainties for a power system with ideal CPL

Sharmila Sumsurooah, Milijana Odavic, *Member, IEEE,* and Serhiy Bozhko, *Member, IEEE*

***Abstract*—Power electronic systems are prone to instability. The problem, generally attributed to the constant power load (CPL) behaviour of their power electronic controlled loads, can become more acute when the systems are subject to parametric uncertainties. The structured singular value (SSV) based μ method has proven to be a reliable approach for assessing the stability robustness of such uncertain systems. Despite its numerous benefits, the μ method is not often applied to electrical power systems (EPS) with multiple uncertainties. This may be due to the mathematical complexity underlying the μ theory. This work aims to make the μ approach more application-friendly by providing clearer insights into the meaning and usefulness of the robust stability measure μ for EPS with multiple parametric uncertainties. This is achieved by presenting a methodology for translating μ analysis results from the frequency domain to the more perceivable uncertain parameters domain. The method directly demonstrates dependences of system stability on uncertain system parameters. Further, it clearly identifies robust stability domains as subsets of the much wider stability domains. The work is based on a representative EPS connected to an ideal CPL. μ analysis predictions are evaluated and validated against analytical results for the example CPL system.**

***Index Terms*—Robust stability analysis, Linear fractional transformation, Structured singular value, μ analysis.**

I. Introduction

Power electronic systems are the foundations of the electrification of land, air and sea vehicles [1]. Their high efficiency and controllability are allowing the rapid development of the more electric transport. The downside is that power electronic controlled loads, due to their constant power load behaviour, are seen in the network as negative impedances and thus can cause severe stability issues within the power system [2], [3], [4], [5], [6]. Moreover, in practice, these power systems are subject to multiple parameter uncertainties which act simultaneously on the system. This may further compromise system stability. It naturally follows that the stability domains within which such systems may operate safely in the face of uncertainties need to be identified, as an aid to designing robustly stable systems especially for safety critical applications.

The classical approaches, that are generally employed to assess small-signal stability of power electronic systems, are the eigenvalue-based method and impedance-based methods such as Middlebrook criterion [7], [8]. A key drawback of classical techniques is that the analysis is based on the nominal model and does not include system uncertainties such as parameter variations. In order to incorporate uncertainties when using classical methods, the eigenvalue method is typically combined with the Monte Carlo simulation. However, this probabilistic stability assessment approach can be employed to determine probability density functions of critical eigenvalues but cannot guarantee to identify the most critical system scenarios with respect to stability [9], [10]. In addition, the study [4] proposes an admittance space stability analysis method that incorporates parametric uncertainties in the application of the classical impedance-based Energy Source Analysis Consortium approach. The aforementioned method involves exhaustive iterations of parameter variations, linearisation at a number of equilibrium points and computation of impedances. The authors in [4] have developed a software to make the process automatic in order to make the approach less laborious. Conversely, the SSV based μ method, that is presented in this work, has proven to produce reliable results in stability assessment of uncertain systems [9], [11], [12], [13]. Further, the μ approach excludes the need for extensive linearisation and parameter iterations.

Important developments in the multivariable control theory since the early eighties have made μ analysis more rigorous and applicable [11], [14], [15]. A great amount of literature is devoted to the theoretical framework. It discusses the modelling technique of linear fractional transformation (LFT), and the computation of μ, which is a measure of stability robustness of the system [16] - [17]. However, despite its numerous advantages, the μ method has a few limitations, which could explain why it is still not as widely used as classical methods. First, the mathematical complexity underlying the SSV theorem [16], [18] is such that certain aspects of the approach are not always fully understood and interpretation thereof may not be evident from the engineering viewpoint. Nonetheless, some works such as [19], [20], [21] have brought to the reader a good understanding of both the theoretical and practical aspects of the μ approach. Further, the significance of the single-valued μ measure, in the analysis of multiple parametric uncertainties, does not seem to have been adequately treated in the literature.

The aim of this work is then to address the above shortcomings by providing deeper insights into the meaning and application of μ value. The work presents certain key aspects of the μ approach in view of making the method more applicable to power electronic systems with multiple uncertainties. This is achieved by developing a methodology for translating the frequency based μ analysis results into the more perceivable parametric domain, for a power system subject to single and multiple uncertainties. In order to keep focus

on the significance and usefulness of μ, a representative EPS connected to the well-established ideal CPL is employed for illustration [3], [5], [6]. μ analysis predictions are evaluated and verified against analytical results.

II. Theoretical Background

An uncertain system is said to have robust stability if it remains stable as all of its uncertain elements vary within their defined ranges. The μ method is an effective tool for evaluating stability robustness of such system models. Prior to μ analysis, the uncertain system must nonetheless be expressed in the LFT form [14] - [22].

LFT is a modelling technique which is employed to "pull out" the indeterminate part from the known part of a system model and place it in the feedback form. If a general uncertain parameter P is considered to be bounded in the region [P_{min}, P_{max}], it may be represented in its normalised form δ_P bounded within $[-1, 1]$. It is easy to show that P can be modelled as an LFT in δ_P in the expression (1) and in the matrix form in Fig. 1.

$$P = P_o + P_o P_{var} \delta_P, \quad \delta_P \in [-1, 1] \tag{1}$$
$$\textit{where} \quad P_o = (P_{min} + P_{max})/2$$
$$\textit{and} \quad P_{var} = (P_{max} - P_{min})/(P_{max} + P_{min})$$

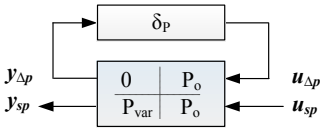

Fig. 1: Uncertain Parameter P as an LFT

Similarly, the model of an entire system with parametric uncertainties can be represented in the LFT form [17], [22]. For the purpose of illustration, a general uncertain system expressed in the state space form with input u and output y, as shown in Fig. 2a, is considered. Based on the technique of LFT, it is possible to extract the set of uncertainties in their normalised form and regroup them in the diagonal uncertainty matrix Δ as shown in Fig. 2b. As a result, the initial state space matrix is expanded to accommodate two sets of inputs namely u_Δ and u_s and two sets of output y_Δ and y_s as shown in Fig. 2b [23], [24], [25]. The expanded state space matrix in Fig. 2b can be converted into the $N\Delta$ configuration in Fig. 2c by absorbing the "states" [24].

The transfer function of the system in Fig. 2c, which is also known as the upper linear fractional transformation, is given by (2). The uncertainty matrix Δ is clearly distinguishable in (2) and is said to have been "pulled out" of the original uncertain system.

$$F_u(N, \Delta) = \frac{y_s}{u_s} = N_{22} + N_{21}\Delta(I - N_{11}\Delta)^{-1}N_{12} \tag{2}$$

For completion, the reader is referred to [24], which examines in detail the technique of LFT through an example resistance-inductance-capacitance (RLC) circuit.

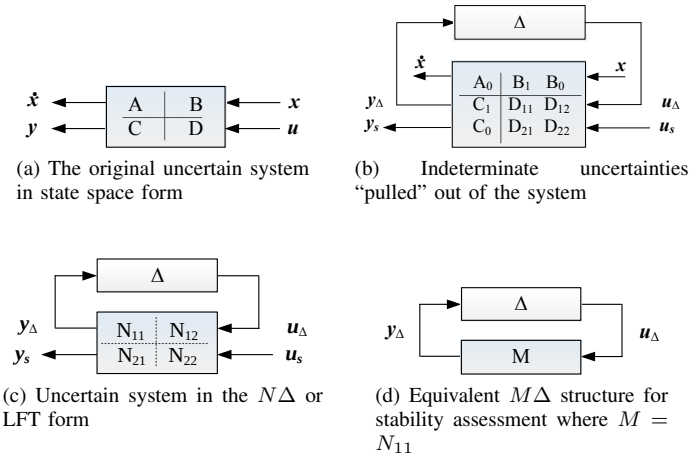

(a) The original uncertain system in state space form

(b) Indeterminate uncertainties "pulled" out of the system

(c) Uncertain system in the $N\Delta$ or LFT form

(d) Equivalent $M\Delta$ structure for stability assessment where $M = N_{11}$

Fig. 2: LFT of an uncertain system

Referring to the general LFT expression (2), it can be seen that the only source that can cause the system $N\Delta$ to become unstable is the feedback term $(I - M\Delta)^{-1}$, where $M = N_{11}$. The system M can be derived as (3) from Fig. 2b [17], [19]. The stability of the whole system (i.e the system $N\Delta$) therefore rests on the stability of the $M\Delta$ structure shown in Fig. 2d.

$$M(s) = N_{11}(s) = C_1(sI - A_0)^{-1}B_1 + D_{11} \tag{3}$$

The robust stability condition for structured uncertainties is given by the structured singular value, as defined in (4) [14] - [22].

$$\mu_\Delta(M(s)) = \frac{1}{min[\bar{\sigma}(\Delta) : det(I - M\Delta) = 0, \Delta\ structured]} \tag{4}$$

The structured singular value, commonly denoted as μ, identifies the smallest perturbation matrix (Δ) that destabilises the system by causing the movement of system poles to the imaginary axis [18], [23]. The SSV theory gives necessary and sufficient conditions for stability robustness [16]. If μ is less than 1, the system is guaranteed to be robustly stable for the entire uncertainty set.

It is computationally hard to obtain the exact value of μ, especially for large size problems, as widely reported in the literature [15], [16], [20]. The solution is to compute a lower bound $\underline{\mu}$ and an upper bound $\bar{\mu}$ rather than the exact value of μ. The lower bound $\underline{\mu}$, as opposed to the upper bound $\bar{\mu}$, is always computed at the boundary of stability. However, it is to be stressed that the lower bound $\underline{\mu}$ may not always be equal to μ and the maximum possible error can be estimated by the gap [$\underline{\mu}$, $\bar{\mu}$] for each case [20]. In fact, the worse ratio of $\underline{\mu}/\bar{\mu}$ has been reported to be equal to 0.85 while for most cases the ratio is close to unity [23].

III. Power System Modelling

A power converter may achieve nearly constant power load regulation under fast controller actions. These types of power

electronic controlled loads can mathematically be represented as ideal CPLs [3], [5], [6], [26]. Fig. 3 depicts the example EPS that is used to support this study. It is an ideal CPL connected to the dc power supply through an input LC filter. The system parameters are defined in Table I.

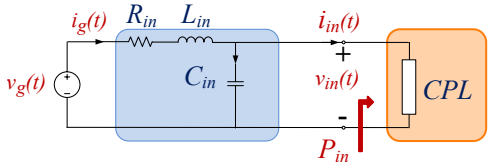

Fig. 3: Non-linear model of the system with ideal CPL

TABLE I: Nominal values for system parameters

Symbol	Units	Nominal values	Description
v_g	V	19.8	DC source voltage
R_{in}	$m\Omega$	160	Input Resistance
L_{in}	μH	511.8	Input filter inductance
C_{in}	μF	95	Input filter capacitance
P_{in}	W	10.4	Input power

The ideal CPL has non-linear characteristics which can be depicted in the non-linear equation (5) and in Fig. 4.

$$i_{in}(t) = \frac{P_{in}}{v_{in}(t)} \tag{5}$$

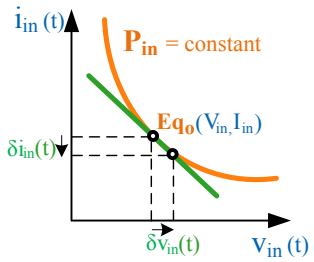

Fig. 4: Characteristic curve of the ideal CPL

At any given operating point, the system currents and voltages of the EPS in Fig. 3 may be represented by dc values with some superimposed small-signal ac components as shown in (6).

$$i_{in}(t) = I_{in} + \hat{i}_{in}(t), \quad v_{in}(t) = V_{in} + \hat{v}_{in}(t) \tag{6}$$

In view of linearising the non-linear model of the CPL at the dc quiescent point (V_{in}, I_{in}) denoted as Eq_o in Fig. 4, the gradient at that point is obtained from the partial derivative of (5). This gradient represents the small-signal incremental impedance at the dc point and is given by (7).

$$\frac{\delta i_{in}(t)}{\delta v_{in}(t)} == \frac{i_{in}(t) - I_{in}}{v_{in}(t) - V_{in}} = \frac{\hat{i}_{in}(t)}{\hat{v}_{in}(t)} = -\frac{P_{in}}{V_{in}^2} \tag{7}$$

It is worth noting that while the instantaneous impedance V_{in}/I_{in} is positive, the small-signal incremental impedance, as given by (7) and shown in Fig. 4, is negative. It is the negative impedance characteristics of the CPLs that account for their propensity to become unstable [6]. Based on this analysis, the small-signal model of the CPL system can be represented in Fig. 5.

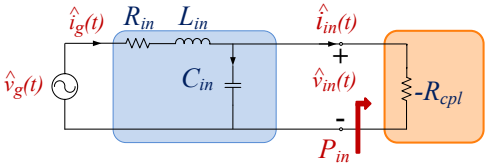

Fig. 5: Small-signal model of the system with ideal CPL

Furthermore, by using tangent line approximation of the non-linear equation (5) together with the small-signal incremental impedance (7), the linear model of the CPL can be obtained as (8). Based on the linear function (8), the corresponding circuit diagram can be constructed by connecting a negative resistance $-R_{cpl}$ in parallel with a constant current source I_{cpl} as shown in Fig. 6.

$$i_{in}(t) = \frac{1}{(-R_{cpl})} v_{in}(t) + I_{cpl} \tag{8}$$
$$where \quad R_{cpl} = -\frac{V_{in}^2}{P_{in}}, \quad I_{cpl} = \frac{2P_{in}}{V_{in}} = 2I_{in}$$

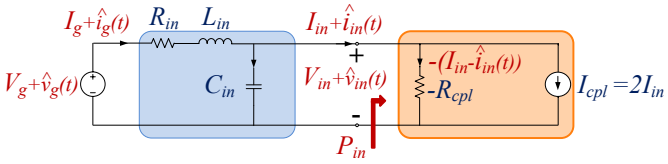

Fig. 6: Linear model of the system with ideal CPL

This paper aims at applying μ analysis to the EPS connected to the ideal CPL, as shown in Fig. 3, over a range of operating points and parameter variations. To this end, the modelling methodology presented in [13] is employed to represent the EPS as an equivalent linear model that contains all system variability, in addition to being suitable for μ analysis. The method is based on symbolic linearisation around an arbitrary equilibrium point.

The first step involves writing the differential equations which describe the dynamic behaviour of the non-linear system in Fig. 3. These are given as (9) and (10).

$$\frac{di_g(t)}{dt} = -\frac{R_{in}}{L_{in}} i_g(t) - \frac{1}{L_{in}} v_{in}(t) + \frac{1}{L_{in}} v_g(t) \tag{9}$$
$$\frac{dv_{in}(t)}{dt} = \frac{1}{C_{in}} i_g(t) - \frac{P_{in}}{C_{in}} \frac{1}{v_{in}(t)} \tag{10}$$

The next step is to linearise the non-linear system model in symbolic form. The equations (9) and (10) are first represented in the state space form (11) with the states $x(t)$=[$i_g(t)$, $v_{in}(t)$], input u(t)= $v_g(t)$ and output $y(t)$=$v_{in}(t)$. For the purpose of linearisation, the system variables are expanded in terms of

their dc and ac components as shown in (11). Linearisation is then performed based on (12) where the dc quiescent point and the small-signal ac model are extracted as (13) and (14) respectively.

$$\dot{x}(t) = f(x,u), \ \textit{where} \quad x(t) = X + \hat{x}(t), \quad u(t) = U + \hat{u}(t) \tag{11}$$

$$\dot{X} + \dot{\hat{x}}(t) \cong f(X,U) + \left[\frac{\delta f}{\delta x}\right]_{X,U} \hat{x}(t) + \left[\frac{\delta f}{\delta u}\right]_{X,U} \hat{u}(t) \tag{12}$$

$$0 = f(X,U) \quad \textit{dc terms} \tag{13}$$

$$\begin{aligned}\dot{\hat{x}}(t) &= \left[\frac{\delta f}{\delta x}\right]_{X,U} \hat{x}(t) + \left[\frac{\delta f}{\delta u}\right]_{X,U} \hat{u}(t) \\ &= A\hat{x}(t) + B\hat{u}(t) \quad \textit{ac terms}\end{aligned} \tag{14}$$

Based on (13) and $U = V_g$, the dc equilibrium states $X = [I_g, V_{in}]$ can be computed by equating (9) - (10) to zero and are given as (15) and (16) respectively.

$$I_g = I_{in} = \frac{P_{in}}{V_{in}} \tag{15}$$

$$V_{in} = \frac{V_g}{2}[1 + \sqrt{1 - 4R_{in}\frac{P_{in}}{V_g^2}}] \tag{16}$$

It is to be noted that all the elements in the system model should be in their rational form in order to allow conversion of the system model in its corresponding LFT configuration [27]. Hence the voltage V_{in} in (16) is expressed in its rational form V_{in-est} as shown in (17) by employing binomial expansion.

$$V_{in-est} = V_g - \frac{R_{in}P_{in}}{V_g} \tag{17}$$

Based on the general equation (14), the small-signal ac model of the considered system can be obtained as (18). Besides, the small-signal output can be written as (19) from $\hat{y}(t) = \hat{v}_{in}(t)$.

$$\begin{bmatrix} \frac{d\hat{i}_g(t)}{dt} \\ \frac{d\hat{v}_{in}(t)}{dt} \end{bmatrix} = \begin{bmatrix} -\frac{R_{in}}{L_{in}} & -\frac{1}{L_{in}} \\ \frac{1}{C_{in}} & -\frac{1}{C_{in}R_{cpl}} \end{bmatrix} \begin{bmatrix} \hat{i}_g(t) \\ \hat{v}_{in}(t) \end{bmatrix} + \begin{bmatrix} \frac{1}{L_{in}} \\ 0 \end{bmatrix} \hat{v}_g(t), \quad \textit{where} \quad R_{cpl} = -\frac{V_{in-est}^2}{P_{in}} \tag{18}$$

$$\hat{y}(t) = \begin{bmatrix} 0 & 1 \end{bmatrix} \begin{bmatrix} \hat{i}_g(t) \\ \hat{v}_{in}(t) \end{bmatrix} \tag{19}$$

The developed small-signal model, (18) - (19), operating about the dc equilibrium point (15) - (16), represents the non-linear system shown in Fig. 3 over a range of operating points and parameter variations, in addition to being suitable for μ analysis [28]. It is referred to as the equivalent linear model of the power system in Fig. 3.

In this work, μ analysis is applied to the equivalent linear model (18) - (19) to evaluate the stability robustness and stability domains of the power system in Fig. 3. The μ predictions are verified against results obtained analytically. To that end, the stability boundary conditions based on the characteristic equations of the power system under study are developed in the next section.

IV. Analytical Assessment of System Stability

The stability of a system can be examined by verifying the location of the roots of its characteristic equation. The characteristic equation of the small-signal model of the power system, as shown in Fig. 5, is given by the denominator of the transfer function (20).

$$\frac{\hat{v}_{in}(t)}{\hat{v}_g(t)} = \frac{1}{[C_{in}L_{in}s^2 + (C_{in}R_{in} - \frac{L_{in}P_{in}}{V_{in-est}^2})s + (1 - \frac{R_{in}P_{in}}{V_{in-est}^2})]} \tag{20}$$

Based on Routh-Hurwitz criterion, the terms in the characteristic equation as given by (21) and (22) must be positive for the system to be stable [29]. However, since the input resistance R_{in} has a relatively low value, condition (22) can be neglected and the main condition for system stability becomes (21).

$$C_{in}R_{in} - \frac{L_{in}P_{in}}{V_{in-est}^2} > 0 \tag{21}$$

$$1 - \frac{R_{in}P_{in}}{V_{in-est}^2} > 0 \tag{22}$$

Hence at boundary stability, the critical power P_{in} is obtained as (23) from the main condition (21). Replacing V_{in-est} in (23) by (17) produces the expression (24) from which the critical value of P_{in} can be computed analytically.

$$P_{in} = \frac{C_{in}R_{in}V_{in-est}^2}{L_{in}} \tag{23}$$

$$\frac{R_{in}^2}{V_g^2}P_{in}^2 - (\frac{L_{in}}{C_{in}R_{in}} + 2R_{in})P_{in} + V_g^2 = 0 \tag{24}$$

Further, the critical frequency of oscillation is given as (25); the expression is derived by substituting (23) in the system characteristic equation in (20) and solving for s or jw. The critical conditions (24) and (25) are used to verify the results from μ analysis.

$$jw = j2\pi f = \sqrt{(\frac{L_{in} - C_{in}R_{in}^2}{C_{in}L_{in}^2})} \tag{25}$$

V. System with Single Parametric Uncertainty

This section demonstrates how μ analysis is employed to determine stability robustness and stability domains of the power system in Fig. 3 when it is subject to variation in a single parameter. The nominal values of the system parameters are given in Table I. Considering that the input power P_{in} may vary within $\pm 33\%$ of its nominal value of $10.4\ W$, as defined in Table II, μ analysis is applied to the equivalent linear model of the power system, given by (18) - (19), to determine the critical or smallest input power that can destabilise the system.

TABLE II: Single uncertain parameter system (case I) - the uncertain parameter

Uncertain parameter	Nominal value	Range of variation
P_{in}	P_{ino} = 10.4 W	P_{invar} = ± 33 %

A. μ analysis

The application of μ analysis requires that the equivalent linear system model be first converted in the LFT form. Although the LFT operation can be done manually, the process can be laborious [24]. Fortunately, the LFT exercise as well as μ analysis can be performed automatically by employing specialised software tools. MATLAB® Robust Stability Toolbox has been used in this work. The operation of LFT entails expressing all uncertain parameters in the system model as LFTs. Thus, the parameter P_{in} in the system model is written in its normalised form δ_{Pin} based on (26) and the information in Table II.

$$P_{in} = P_{ino} + P_{ino}\ P_{invar}\ \delta_{Pin} \tag{26}$$

The normalised parameters δ_{Pin} are then extracted from the system model (18) - (19) and grouped in a diagonal matrix in a feedback form by employing the LFT technique. This results in the system model being converted in the LFT form with the disturbance matrix given by (27); δ_{Pin} appears 3 times in the uncertainty matrix since P_{in} appears that number of times in the uncertain system model.

$$\Delta(j2\pi f) = diag(\delta_{Pin}\ I_3) \tag{27}$$

The system stability can now be examined by applying μ analysis to the system model in the LFT form. Based on the principle of SSV, μ analysis identifies the smallest uncertainty matrix that destabilises the system. The results are depicted in Fig. 7a and 7b.

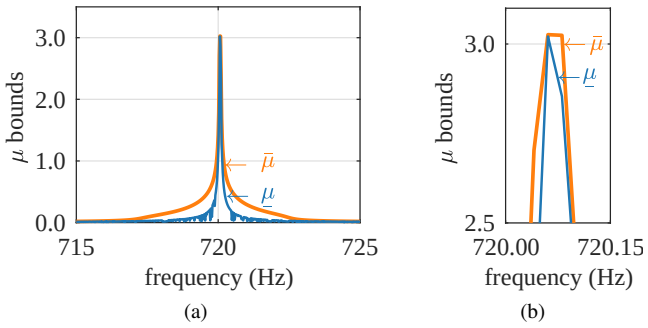

Fig. 7: Single uncertain parameter system (a) μ chart to predict critical P_{in} (b) zoomed area near peak of μ chart

Of note is that the systems N and M, as defined in Fig. 2c and 2d, can be extracted from the μ analysis results in the numerical form rather than the symbolic form at the boundary of stability. For this case study, the systems N and M can be obtained from the expanded state space matrix in the form of Fig. 2b given in the appendix A.

From the μ chart, it can be seen that the peak values of both the lower bound $\underline{\mu}$ and the upper bound $\bar{\mu}$ are equal to 3.02 at the frequency of 720 Hz. The critical frequency corresponds to the resonant frequency of the LC filter which can be estimated as $1/2\pi\sqrt{L_{in}C_{in}}$. By using appropriate function in MATLAB® Robust Stability Toolbox, the smallest destabilising disturbance matrix is extracted as $\Delta(j2\pi720)$ as shown in (28) and in Table III [21].

$$\Delta(j2\pi720) = diag(+0.331\ I_3) \tag{28}$$

The critical value of δ_{Pin} is equal to 0.331 as can be deduced by comparing $\Delta(j2\pi720)$ in (28) with the structure of the uncertainty matrix in (27). The robust stability margin can be calculated as $1/\mu = 0.331$. The smallest input power that can destabilise the system is computed as 11.53 W based on critical δ_{Pin} and equation (26), as shown in Table III.

TABLE III: Single uncertain parameter system - μ analysis results

Perturbation matrix	$\bar{\sigma}(\Delta(jw))$	$\mu = 1/\bar{\sigma}(\Delta(jw))$	Critical P_{in}
$\Delta(j2\pi720)$	0.331	3.02	11.53 W

B. Analytical verification

The critical power and frequency can be calculated according to the analytical stability conditions (24) and (25) respectively. The analytical results agree with the μ analysis results as shown in Table IV. This finding supports the results from μ analysis.

TABLE IV: Single uncertain parameter system - μ analysis and analytical results

	μ analysis results	Analytical results
Critical input power (P_{in})	11.53 W	11.53 W
Critical frequency (f)	720 Hz	720 Hz

C. Robust stability domain

The μ tool identifies the smallest destabilising perturbation matrix as given in (28). In parametric space, this represents the largest normalised line segment of coordinate size $1/\mu$ with respect to the nominal point, within which the system is guaranteed robustly stable. For this case study, the line segment, of coordinate size $1/\mu = 0.331$, is represented in Fig. 8. This implies that for any value of $\mid \delta_{Pin} \mid < 0.331$, the system is guaranteed robustly stable. In contrast for any value of $\delta_{Pin} > +0.331$ the system is unstable in accordance with (28).

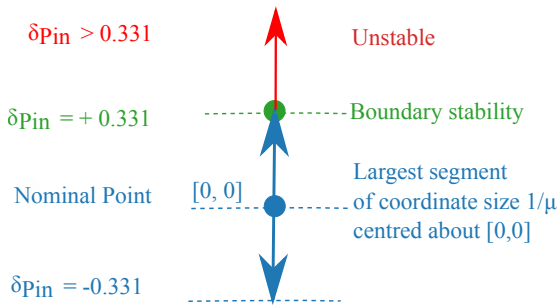

Fig. 8: Single uncertain parameter system - Largest linear segment of coordinate size $(1/\mu)$ centred about nominal point within which system is robustly stable

VI. System with two parametric uncertainties

In this case study, the power system in Fig. 3 is subject to variation in two parameters namely C_{in} and P_{in}, as depicted in Table V. The other parameters are fixed as defined in Table I. This subsection examines both the stability robustness and the stability domain of the system.

TABLE V: Two uncertain parameters system (case II) - the uncertain parameters

Uncertain parameters	Nominal value	Range of variation
P_{in}	P_{ino} = 10.4 W	P_{invar} = ± 33 %
C_{in}	C_{ino} = 95 μF	C_{invar} = ± 10 %

A. μ analysis

μ analysis is performed on the equivalent linear model (18) - (19) based on the nominal values and the range of variation of the two uncertain parameters as defined in Table V. The resulting μ chart is depicted in Fig. 9a and 9b, from which it can be noted that μ=$\underline{\mu}$=$\bar{\mu}$=4.03.

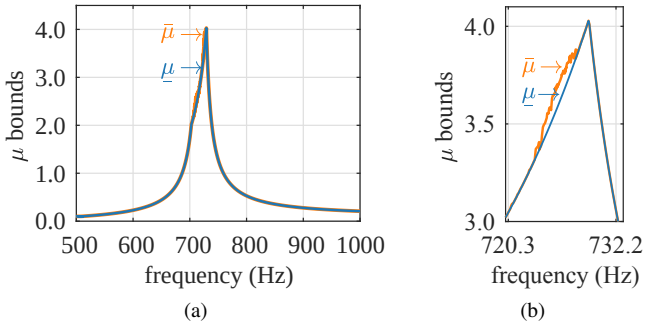

Fig. 9: Two uncertain parameters system (a) μ chart to determine critical C_{in} and P_{in} (b) zoomed area near peak of μ chart

The structure of the uncertainty matrix is obtained as (29) from the LFT operation. The smallest perturbation matrix which is provided by μ analysis at the critical frequency of 729.2 Hz is given in (30) .

$$\Delta(j2\pi f) = diag(\delta_{Cin}\ I_2,\ \delta_{Pin}\ I_3) \tag{29}$$
$$\Delta(j2\pi 729.2) = diag(-0.248\ I_2,\ +0.248\ I_3) \tag{30}$$

By comparing the perturbation matrix (30) with the structure of the uncertainty matrix (29), the critical values of δ_{Cin} and δ_{Pin} can be obtained, as shown in Table VI. Based on these critical values, the smallest destabilising input capacitance and input power are computed as 92.65 μF and 11.25 W respectively, as shown in Table VI.

B. Analytical verification

For verifying the μ results, the input power and frequency are computed from the analytical stability boundary conditions (24) and (25) respectively with C_{in} set to its critical value of 92.65 μF. The analytically obtained results are found to match the μ analysis results as shown in Table VII.

TABLE VI: Two uncertain parameters system - Critical values of C_{in}, P_{in} determined from μ analysis

Critical $\Delta(jw)$	δC_{in}	δP_{in}	C_{in} (μF)	P_{in} (W)
$\Delta(j2\pi 729.2)$	-0.248	+0.248	92.65	11.25

TABLE VII: Two uncertain parameters system - μ analysis and analytical results

	μ analysis results	Analytical results
Critical input power (P_{in})	11.25 W	11.25 W
Critical frequency (f)	729.2 Hz	729.2 Hz

C. Stability domains

This section demonstrates how μ analysis can be used to determine stability domains of the power system under study. As discussed earlier, the peak value of μ corresponds to a perturbation matrix at the critical frequency of 729.2 Hz. Similarly, each point along the μ chart corresponds to a particular perturbation matrix at a specific frequency. These perturbation matrices can be extracted from the μ chart and employed to construct stability domains of the considered system [21]. For this case study, perturbation matrices are extracted at a number of frequency points on the μ chart shown in Fig. 10.

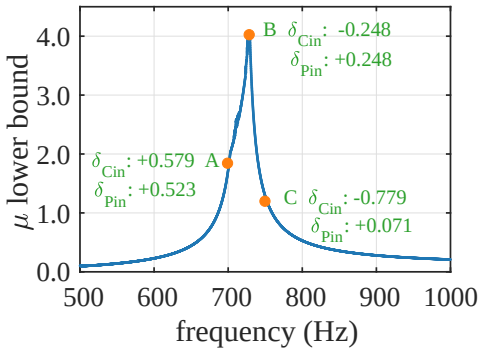

Fig. 10: Two uncertain parameters system - Points A, B, C chosen to illustrate construction of stability domain

For the purpose of illustration, three uncertainty matrices corresponding to points A, B and C in Fig. 10, and given by (31), (30) (32) respectively are analysed. The corresponding μ values are given in Table VIII.

$$\Delta(j2\pi 700) = diag(+0.579\ I_2,\ +0.523\ I_3) \tag{31}$$
$$\Delta(j2\pi 750) = diag(-0.779\ I_2,\ +0.071\ I_3) \tag{32}$$

TABLE VIII: Two uncertain parameters system - μ lower bound for points A, B and C

Points	Perturbation Matrix $\Delta(jw)$	$\bar{\sigma}(\Delta(jw))$	μ = 1/$\bar{\sigma}(\Delta(jw))$
A	$\Delta(j2\pi 700.0)$	0.579	1.73
B	$\Delta(j2\pi 729.2)$	0.248	4.03
C	$\Delta(j2\pi 750.0)$	0.779	1.28

The next step involves identifying the values of δ_{Cin} and δ_{Pin} from the extracted perturbation matrices based on the structure of the uncertainty matrix (29). The normalised parameters are then converted into their actual values C_{in} and P_{in}, based on (26). The corresponding values for matrices A, B and C are depicted in Table IX.

TABLE IX: Two uncertain parameters system - Critical destabilising parameter values for points A, B and C

Perturbation Matrix	δC_{in}	δP_{in}	C_{in} (μF)	P_{in} (W)
A $\Delta(j2\pi 700.0)$	+0.579	+0.523	100.5	12.2
B $\Delta(j2\pi 729.2)$	-0.248	+0.248	92.6	11.3
C $\Delta(j2\pi 750.0)$	-0.779	+0.071	87.6	10.6

Finally, the critical values of P_{in} are plotted against the critical values of C_{in}. Fig. 11 shows the resulting stability line. The points A, B and C shown in Fig. 11 serve to demonstrate how the μ chart has been 'translated' into a stability line.

In order to verify the validity of the stability line obtained from μ analysis, the input power P_{in} is computed for a number of values of C_{in} in the range [85.5 μF, 104.5 μF] based on the analytical equation (24). The resulting plot of C_{in} against P_{in} is shown in Fig. 11. The boundary stability curve obtained from the analytical method matches the curve generated from μ analysis as can be noted from Fig. 11. These findings validate the μ analysis results.

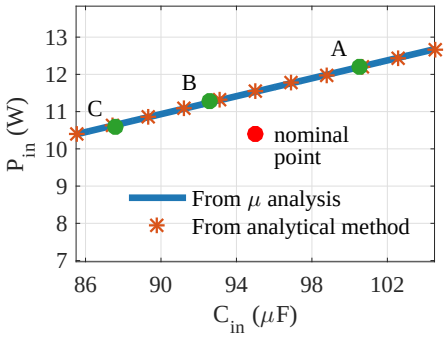

Fig. 11: Two uncertain parameters system - stability domain from μ analysis and analytical method

D. Analysis of robust stability domains

For this case study, the robust stability margin $(1/\mu)$ equals 0.248. In parametric space and for a system subject to two parametric uncertainties, the μ approach identifies the largest square of coordinate size $1/\mu$ within which the system can be guaranteed robustly stable [20]. In order to illustrate this point, the squares connecting points A, B, C are drawn centred about the nominal point (0,0), as shown in Fig. 12a, 12b and 12c respectively.

The rectangle encompassing point A falls in both the stable and unstable regions. In contrast, the 'square' connecting point 'B' is completely in the stable region. Point B corresponds to the peak value of μ. Of note is that although the rectangle connecting point 'C' falls entirely in the stable region, it does not give the largest uncertainty size for all uncertain

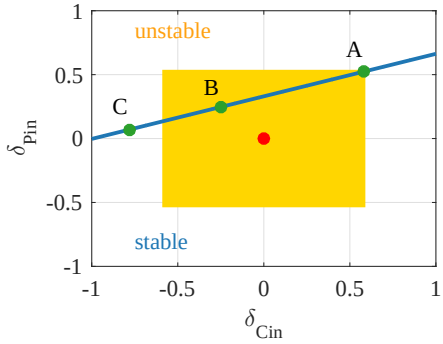

(a) Rectangle centred about nominal point, connecting point A

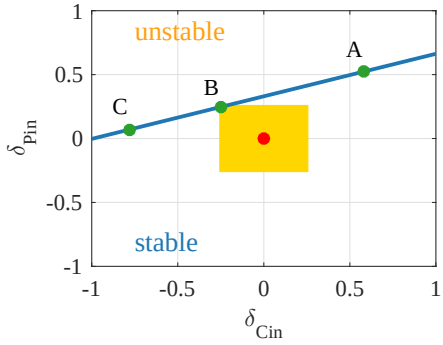

(b) Largest square of coordinate size $(1/\mu)$ centred about nominal point within which system is robustly stable

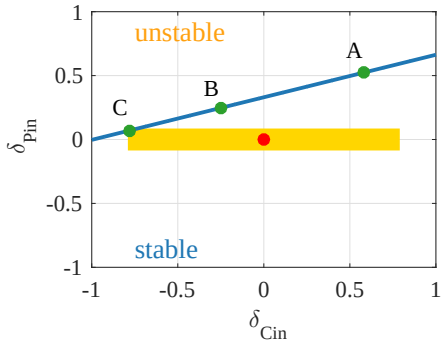

(c) Rectangle centred about nominal point, connecting point C

Fig. 12: Two uncertain parameters system

parameters, for which robust stability is guaranteed. Hence, in order to guarantee robust stability of the system, uncertainties have to stay within the 'square' region identified in Fig. 12b.

VII. System with three parametric uncertainties

This section assesses stability robustness of the power system under study when it is subject to three parametric uncertainties as defined in Table X. It also provides an insight into the meaning of μ by exploring the stability domains.

A. μ analysis

After defining the uncertain system parameters C_{in}, L_{in} and P_{in} as in Table X, robust stability is analysed using the μ tool.

TABLE X: Three uncertain parameters system (case III) - the uncertain parameters

Uncertain parameters	Nominal value	Range of variation
P_{in}	P_{ino} = 10.4 W	P_{invar} = $\pm$ 33 %
C_{in}	C_{ino} = 95 μF	C_{invar} = $\pm$ 10 %
L_{in}	L_{ino} = 511.8 μH	L_{invar} = $\pm$ 10 %

The μ chart is shown in Fig. 13a and fig. 13b. The maximum value of the μ lower bound is 4.974 and is nearly equal to that of the μ upper bound.

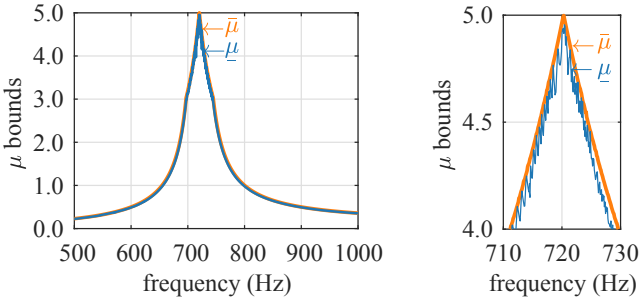

Fig. 13: Three uncertain parameters system (a) μ chart to determine critical C_{in}, L_{in}, P_{in} (b) zoomed area near peak of μ chart

The structure of the uncertainty matrix, as extracted from μ analysis, is shown in (33). The critical uncertain matrix at the critical frequency of 720.5 Hz is shown in (34).

$$\Delta(j2\pi f) = diag(\delta_{Cin}\ I_2,\ \delta_{Lin}\ I_1,\ \delta_{Pin}\ I_3) \quad (33)$$

$$\Delta(j2\pi 720.5) = diag(-0.201\ I_2,\ +0.196\ I_1,\ +0.201\ I_3) \quad (34)$$

The values of δ_{Cin}, δ_{Lin}, δ_{Pin} pertaining to the critical uncertainty matrix can be obtained by comparing the elements of $\Delta(j2\pi 720.5)$ in (34) with the elements in (33), and are shown in Table XI. Further, the smallest parameter values that can destabilise the power system can be computed from these normalised values and the general LFT expression (26), as depicted in Table XI.

TABLE XI: Three uncertain parameters system - Critical values of C_{in}, L_{in}, P_{in} from μ analysis

δC_{in}	δL_{in}	δP_{in}	C_{in} (μF)	L_{in} (mH)	P_{in} (W)
-0.201	+0.196	+0.201	93.1	521.8	11.1

B. Analytical verification

In order to verify the μ analysis results in Table XI, the input power P_{in} and frequency f are computed from the analytical equations (24) - (25), with C_{in} and L_{in} set to the critical values of 93.1 μF and 521.8 mH respectively. The analytical results match μ analysis predictions as shown in Table XII. This confirms that μ analysis has identified critical parameters at the boundary of stability for the case study.

TABLE XII: Three uncertain parameters system - μ analysis and analytical results of critical P_{in} and f

	μ analysis results	Analytical results
Critical input power (P_{in})	11.1 W	11.1 W
Critical frequency (f)	720.5 Hz	720.5 Hz

C. Stability domains

This subsection translates frequency-based μ results into parametric space. It provides insights into the usefulness of μ in the identification of the parametric space within which a system is guaranteed robustly stable.

1) μ in parametric space: In order to generate the stability domain of the power system under consideration, perturbation matrices are firstly extracted at a number of frequency points on the chart of the μ lower bound shown in Fig. 14. For the purpose of illustration, three uncertainty matrices corresponding to the points A, B and C in Fig. 14, and given in (35), (34) and (36) respectively, are analysed.

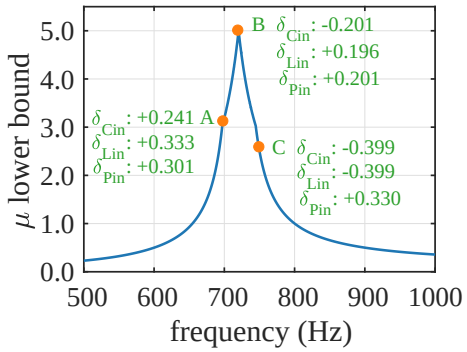

Fig. 14: Three uncertain parameters system - Points A, B, C chosen to illustrate construction of stability domains

$$\Delta(j2\pi 700) = diag(+0.241\ I_2,\ +0.333\ I_1,\ +0.301\ I_3) \quad (35)$$

$$\Delta(j2\pi 750) = diag(-0.399\ I_2,\ -0.399\ I_1,\ +0.330\ I_3) \quad (36)$$

The next step involves identifying the values of δ_{Cin}, δ_{Lin} and δ_{Pin} for each of the perturbation matrices. This is done by comparing the elements of the matrices with the elements of the general uncertainty matrix (33). The normalised parameter values for points A, B and C are given in Table XIII along with the corresponding computed values of C_{in}, L_{in} and P_{in}.

TABLE XIII: Three uncertain parameters system - Critical destabilising parameter values for points A, B and C

	δC_{in}	δL_{in}	δP_{in}	C_{in} (μF)	L_{in} (mH)	P_{in} (W)
A	+0.241	+0.333	+0.301	97.3	528.9	11.4
B	-0.201	+0.196	+0.201	93.1	521.8	11.1
C	-0.399	-0.399	+0.330	91.2	491.4	11.5

The coordinates (δ_{Cin}, δ_{Lin}, δ_{Pin}), extracted from the μ chart, are then plotted in three dimensional space. The resulting chart is depicted in Fig. 15. The points A, B and C shown in Fig. 15 serve to demonstrate how the μ chart in Fig. 14 has been 'translated' from frequency domain to parametric space.

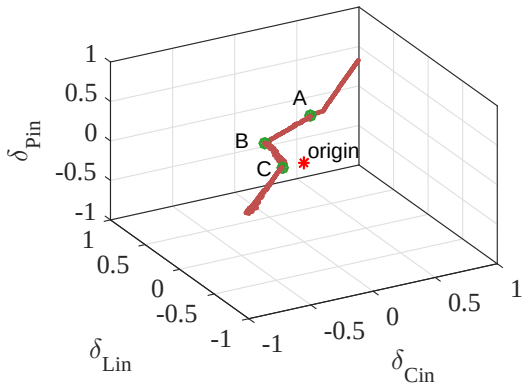

Fig. 15: Three uncertain parameters system - μ lower bound chart translated into parametric space

2) Stability plane from analytical method: In order to gain more insight into the μ approach, in this subsection the stability domains for the system under study are first determined through the analytical method and then correlated with the μ lower bound chart.

A series of points (C_{in}, L_{in}) are chosen in the range of $C_{in} = 95\ \mu F \pm 10\%$ and $L_{in} = 511.8\ mH \pm 10\%$; then P_{in} is calculated iteratively for each coordinate point according to (23). The resulting coordinates (C_{in}, L_{in}, P_{in}) are then converted into their normalised form (δ_{cin}, δ_{Lin}, δ_{Pin}) using the generic equation (26) and the parameter values in Table I. The three-dimensional plot of the coordinates, as shown in Fig. 16, is the boundary stability plane for the system under study. The system is stable for all sets of parameters chosen in the region below the stability plane and is unstable for all sets of parameters chosen in the region above the stability plane.

When the μ lower bound chart in Fig. 15 is superimposed on the analytically obtained stability plane, it is found to lie exactly on the plane as shown in Fig. 16. This proves that the critical parameters determined by the μ lower bound for this case study lie at the boundary of stability.

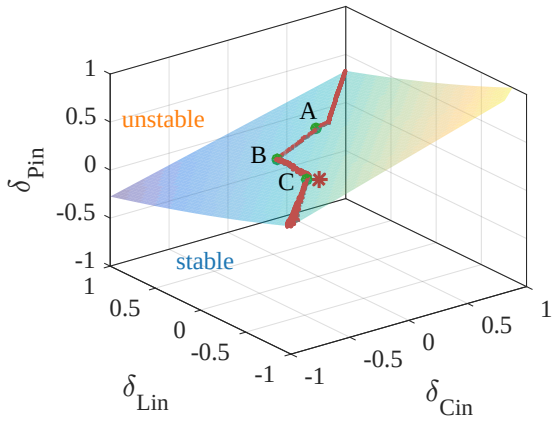

Fig. 16: Three uncertain parameters system - stability boundary plane obtained from analytical method and μ chart translated into parametric space

3) Significance of μ in frequency domain: As can be seen in Fig. 16, the μ chart connects only few of the parameter coordinates within the wide stability plane. This is because the employed algorithm does not verify all the points of the stability plane. Instead, it monitors the boundary stability for migration of those poles, which correspond to the smallest destabilising uncertainty matrices, at every frequency point within the grid. The smallest of all the destabilising perturbation matrices over the entire frequency grid gives $1/\mu$, in accordance with (4). In order to demonstrate this point, this subsection computes μ from the parameter coordinates in the analytical plane in Fig. 16. The procedure employed is based on the definition of μ in (4), which states that $\mu_{\Delta}(M(jw))$ = $1/min[\bar{\sigma}(\Delta(jw))]$. The steps are outlined in Fig. 17 and illustrated below.

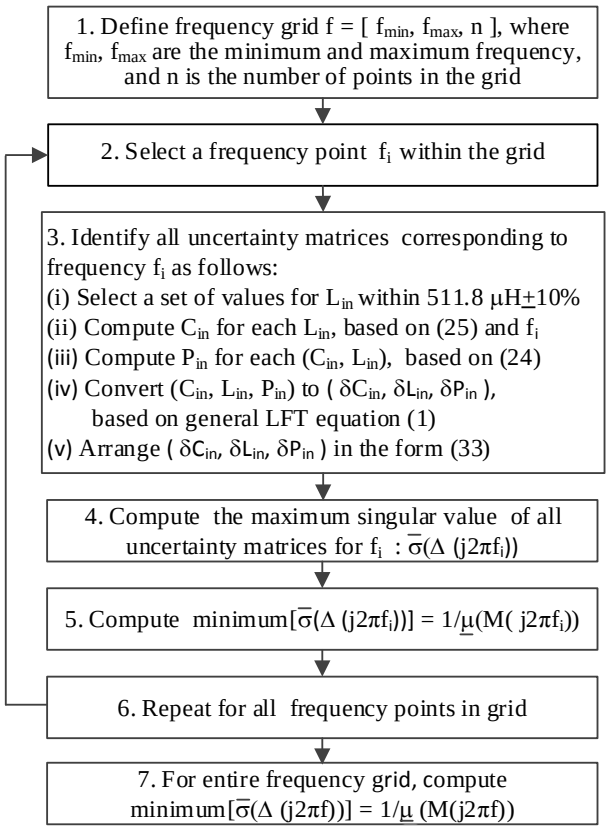

Fig. 17: Flow chart for computing the smallest critical uncertainty matrix for a given system frequency

1) A frequency grid is chosen as a set of 100 points spaced between 500 Hz and 1000 Hz.
2) A frequency of 700 Hz is selected for analysis.
3) A number of uncertainty matrices corresponding to coordinates (δ_{Cin}, δ_{Lin}, δ_{Pin}) and pertaining to 700 Hz are computed. These coordinates, plotted in Fig. 18a, are shown to lie exactly on the stability plane.
4) The maximum singular value of each of the uncertainty matrices, lying on the frequency line of 700 Hz, is computed. For illustration, the maximum singular value

is computed for three points, denoted as 1, 2 and 3 in Fig. 18a, as shown in Table XIV.

5) The smallest uncertainty matrix on the frequency curve 700 Hz is then identified. This corresponds to point 2 which matches point A on the $\underline{\mu}$ chart in Fig. 15, as shown in Table XIV. Hence, the critical perturbation matrix at a given frequency point on the $\underline{\mu}$ chart is found to be the smallest uncertainty matrix that can destabilise the system at that frequency.
6) The above exercise is repeated for all frequency points within the grid. The smallest matrix on the frequency lines 720.5 Hz and 750 Hz correspond to points B and C respectively as shown in Fig. 18a and in Table XV.
7) When all the computed uncertainty matrices on the μ chart are analysed, it is found that the smallest matrix over the entire frequency grid corresponds to point B or the peak of the μ chart. This is shown in Table XVI.

TABLE XIV: Three uncertain parameters system -maximum singular value of matrices 1, 2 and 3 on frequency curve 700 Hz

Points	δC_{in}	δL_{in}	δP_{in}	$\bar{\sigma}(\Delta(j2\pi 700))$	$min[\bar{\sigma}(\Delta(j2\pi 700))]$
1	+0.869	-0.270	+0.720	0.869	-
2	+0.244	+0.330	+0.303	0.330	0.330
3	-0.243	+0.850	-0.005	0.850	-

TABLE XV: Three uncertain parameters system - smallest matrices on frequency lines 700 Hz, 720.5 Hz and 750 Hz

frequency	(δC_{in}, δL_{in}, δP_{in})	$\bar{\sigma}(\Delta(j2\pi f))$	$\mu_{\Delta}(M(j2\pi f))$
700 Hz	A (+0.241, +0.333, +0.301)	0.333	3.00
720.5 Hz	B (-0.201, +0.196, +0.201)	0.201	4.97
750 Hz	C (-0.399, +0.399, +0.330)	0.399	2.51

TABLE XVI: Three uncertain parameters system - μ computed from coordinate points on stability plane

Frequency (f)	$min[\bar{\sigma}(\Delta(j2\pi f))]$	$\mu_{\Delta}(M(j2\pi f))$ =1/min$[\bar{\sigma}(\Delta(j2\pi f))]$
500 Hz - 1000 Hz	0.201	4.97

D. Robust stability domains

Following the analysis in the earlier subsection, the smallest destabilising perturbation matrix on the boundary stability plane corresponds to point B on the μ chart. This can be noted by comparing the sizes of the uncertainty matrices A, B and C in Table XV. The peak value of the μ plot thus provides the largest perturbation matrix that the system is robustly stable against over the entire frequency grid. With respect to parametric space, $\bar{\sigma}(\Delta(jw)) = 1/\mu$ can be interpreted as the coordinate size of the largest cube centred around the nominal point $(0, 0, 0)$ inside of which the system is guaranteed robustly stable.

For the purpose of illustration, a set of rectangular cuboids centred about the nominal point (0,0,0) are drawn to connect points A, B and C respectively. From Fig. 18b, it can be noted that the cuboid connecting point A falls in both the stable and the unstable regions. This is also the case for point C. In contrast, the cube of coordinate size $1/\mu = 0.201$ connecting point B lies totally in the stable region below the stability plane as depicted in Figs. 18c and 18d. It is to be pointed out that the small yet noticeable discrepancies in the normalised values in the uncertainty matrix (34) of point B have been neglected and attributed to numerical inaccuracies. The system is robustly stable for all variations in uncertainties that may occur within the cube in Fig. 18c and 18d. Hence, the μ approach identifies the largest 'cube' in the three dimensional parametric space inside which the system is guaranteed to be robustly stable.

VIII. System with Multiple Parameters Uncertainties

By extrapolating on the ideas presented in the earlier sections, for a system subject to N parametric uncertainties, μ analysis provides the largest hypercube of dimension N centred about the nominal point and of coordinate size $1/\mu$, within which system robust stability can be guaranteed [20]. For a single parametric uncertainty, the hypercube becomes the largest line segment within which the system is guaranteed robustly stable. The line segment is of coordinate size $1/\mu = 0.331$ for case study I. Similarly, when two parametric uncertainties are considered, the hypercube becomes the largest square in the unit bound normalised parameter space within which system robust stability is guaranteed; in case study II this is a square of coordinate size $1/\mu = 0.248$. When considering a system subject to three parametric uncertainties, μ analysis identifies the largest cube within which system robust stability is guaranteed, which in case study III is of coordinate size $1/\mu = 0.201$. Of note is that the initial selection of the nominal values as well as the interval of parameter variations will influence the outcome of the robust stability assessment of a system.

It is interesting to note that the coordinate size of the 'hypercube' or $1/\mu$ tends to decrease with increasing number of uncertainties, as depicted in Table XVII. This clearly shows that stability assessment, if performed without duly incorporating potential system uncertainties, can lead to conservative and possibly erroneous stability margins.

TABLE XVII: Variation of robust stability margin with number of uncertain parameters

Number of parametric uncertainties	Robust stability margin ($1/\mu$)	Critical power (P_{in})
1	0.331	11.53 W
2	0.248	11.25 W
3	0.201	11.10 W

IX. Conclusion

The μ approach is a reliable and effective method that can be adopted for the robust stability analysis of power electronic systems. Yet the μ tool is not widely employed for EPS with multiple parametric uncertainties. This may be attributed to the mathematical complexity of the μ theory. With the aim to

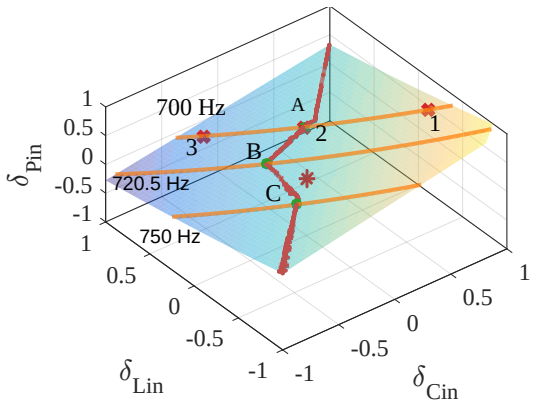

(a) Frequency curve for 700 Hz, 720.5 Hz and 750 Hz on stability boundary plane, obtained from analytical method

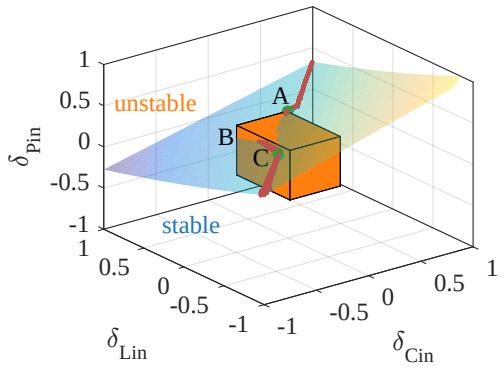

(b) Part of the cuboid centred about the origin and connecting point A falls in the unstable region

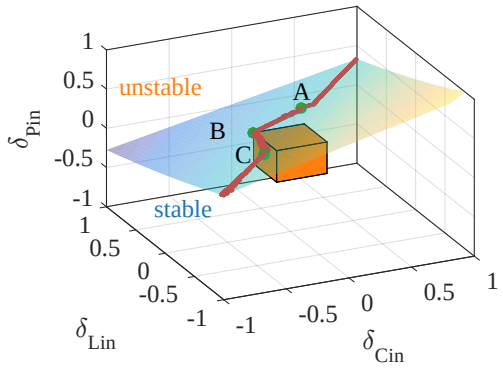

(c) Largest cube of coordinate size $(1/\mu)$ centred about nominal point, connecting point B within which system is stable

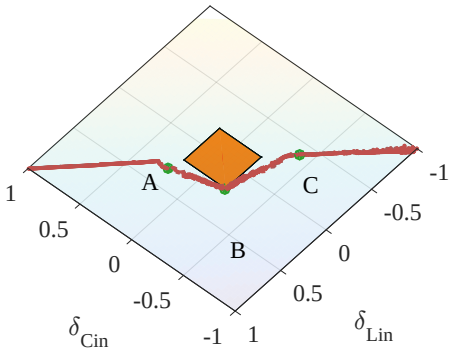

(d) Cube centred about the origin and connecting point B - Top view

Fig. 18: Three uncertain parameters system

make the μ approach more applicable, the work has provided a comprehensive understanding of the robust stability measure μ with respect to single and multiple parametric uncertainties. This has been achieved by applying the μ tool to identify the robust stability domains of the representative EPS connected to an ideal CPL. The work has presented a methodology for translating the μ analysis results from the frequency domain to the more perceivable uncertain parameters domain. It has demonstrated how, for a system subject to N parametric uncertainties, μ provides the largest hypercube of dimension$N$, centred about the nominal point and of coordinate size $1/\mu$, within which the system can be guaranteed robustly stable. Further, it has shown the robust stability domains as subsets of the wider stability domains in the multi-dimensional parametric space. This work has many practical implications. It offers the design engineer a parametric space within which to manoeuvre and choose optimum parameters while ensuring stability robustness. This work has clearly presented certain key aspects of the μ approach in a manner comprehensible enough to make it more application-friendly while offering the possibility of it being extended to more complex studies.

APPENDIX A
EXPANDED STATE SPACE MATRIX N FOR SYSTEM WITH SINGLE PARAMETRIC UNCERTAINTY

$$N = \left[\begin{array}{cc|ccc|c} -312.6 & -1954 & 0 & 0 & 0 & 1954 \\ 1.053e+04 & 281.6 & 1.853 & 0.00793 & 0.1564 & 0 \\ \hline 0 & 50.17 & 0 & 0.001413 & 0.02785 & 0 \\ 0 & 49.95 & 0 & 0.001407 & 0 & 0 \\ 0 & 2.534 & 0 & 7.135e-05 & 0.001407 & 0 \\ \hline 0 & 1 & 0 & 0 & 0 & 0 \end{array}\right] \quad (37)$$

ACKNOWLEDGMENT

The authors gratefully acknowledge the support for the work from the EU as part of the Clean Sky project, part of EU FP7 program.

REFERENCES

[1] I. Moir and A. Seabridge, *Aircraft systems: mechanical, electrical and avionics subsystems integration*, vol. 52. John Wiley & Sons, 2011.
[2] R. D. Middlebrook, "Input filter considerations in design and application of switching regulators," *IAS Record, 1976*, 1976.

[3] A. B. Jusoh, "The instability effect of constant power loads," in *Power and Energy Conference, 2004. PECon 2004. Proceedings. National*, pp. 175–179, IEEE, 2004.
[4] S. D. Sudhoff, S. F. Glover, P. T. Lamm, D. H. Schmucker, and D. Delisle, "Admittance space stability analysis of power electronic systems," *Aerospace and Electronic Systems, IEEE Transactions on*, vol. 36, no. 3, pp. 965–973, 2000.
[5] A. Emadi, A. Khaligh, C. H. Rivetta, and G. A. Williamson, "Constant power loads and negative impedance instability in automotive systems: definition, modeling, stability, and control of power electronic converters and motor drives," *IEEE Transactions on Vehicular Technology*, vol. 55, pp. 1112–1125, July 2006.
[6] A. M. Rahimi and A. Emadi, "An analytical investigation of dc/dc power electronic converters with constant power loads in vehicular power systems," *Vehicular Technology, IEEE Transactions on*, vol. 58, no. 6, pp. 2689–2702, 2009.
[7] G. F. Franklin, J. D. Powell, A. Emami-Naeini, and J. D. Powell, *Feedback control of dynamic systems*, vol. 2. Addison-Wesley Reading, 1994.
[8] R. C. Dorf and R. H. Bishop, "Modern control systems," 1998.
[9] M. Kuhn, Y. Ji, and D. Schrder, "Stability studies of critical DC power system component for More Electric Aircraft using mu sensitivity," in *Control & Automation, 2007. MED'07. Mediterranean Conference on*, pp. 1–6, IEEE, 2007.
[10] J. Elizondo, R. Y. Zhang, J. K. White, and J. L. Kirtley, "Robust small signal stability for microgrids under uncertainty," in *Power Electronics for Distributed Generation Systems (PEDG), 2015 IEEE 6th International Symposium on*, pp. 1–8, IEEE, 2015.
[11] P. M. Young, M. P. Newlin, and J. C. Doyle, "μ analysis with real parametric uncertainty," in *Decision and Control, 1991., Proceedings of the 30th IEEE Conference on*, pp. 1251–1256, IEEE, 1991.
[12] S. Sumsurooah, M. Odavic, S. Bozhko, and D. Boroyevich, "Stability and robustness analysis of a dc/dc power conversion system under operating conditions uncertainties," in *Industrial Electronics Society, IECON 2015 - 41st Annual Conference of the IEEE*, pp. 003110–003115, Nov 2015.
[13] S. Sumsurooah, M. Odavic, and S. Bozhko, "A modeling methodology for robust stability analysis of nonlinear electrical power systems under parameter uncertainties," *IEEE Transactions on Industry Applications*, vol. 52, pp. 4416–4425, Sept 2016.
[14] J. C. Doyle, B. A. Francis, and A. Tannenbaum, *Feedback control theory*, vol. 1. Macmillan Publishing Company New York, 1992.
[15] A. Packard and J. Doyle, "The complex structured singular value," *Automatica*, vol. 29, no. 1, pp. 71–109, 1993.
[16] J. Doyle, "Analysis of feedback systems with structured uncertainties," in *IEE Proceedings D (Control Theory and Applications)*, vol. 129, pp. 242–250, IET, 1982.
[17] S. Skogestad and I. Postlethwaite, *Multivariable feedback control: analysis and design*, vol. 2. Wiley New York, 2007.
[18] M. Green and D. J. Limebeer, *Linear robust control*. Courier Corporation, 2012.
[19] D.-W. Gu, *Robust control design with MATLAB®*, vol. 1. Springer Science & Business Media, 2005.
[20] G. Ferreres, *A practical approach to robustness analysis with aeronautical applications*. Springer Science & Business Media, 1999.
[21] G. Balas, R. Chiang, A. Packard, and M. Safonov, "Robust Control Toolbox 3," 2005.
[22] G. J. Balas, J. C. Doyle, K. Glover, A. Packard, and R. Smith, "μ-analysis and synthesis toolbox: For use with matlab," 2001.
[23] K. Zhou, J. C. Doyle, K. Glover, *et al.*, *Robust and optimal control*, vol. 40. Prentice hall New Jersey, 1996.
[24] S. Sumsurooah, M. Odavic, and D. Boroyevich, "Modelling and robust stability analysis of uncertain systems," in *Proceedings of the 2013 Grand Challenges on Modeling and Simulation Conference*, p. 13, Society for Modeling & Simulation International, 2013.
[25] R. Castellanos, C. Juarez, J. Hernandez, and A. Messina, "Robustness analysis of large power systems with parametric uncertainties," in *Power Engineering Society General Meeting, 2006. IEEE*, pp. 8–pp, IEEE.
[26] K. Areerak, *Modelling and stability analysis of aircraft power systems*. PhD thesis, University of Nottingham, 2009.
[27] A. Varga, G. Looye, D. Moormann, and G. Gräbel, "Automated generation of LFT-based parametric uncertainty descriptions from generic aircraft models," *Mathematical and Computer Modelling of Dynamical Systems*, vol. 4, no. 4, pp. 249–274, 1998.
[28] S. Sumsurooah, M. Odavic, and S. Bozhko, "Development of LFT-based models for robust stability analysis of a generic electrical power system over all operating conditions," in *Electrical Systems for Aircraft, Railway, Ship Propulsion and Road Vehicles (ESARS), 2015 International Conference on*, pp. 1–6, IEEE, 2015.
[29] J. Flower, C. Hodge, and Honorary, "Stability and transient-behavioural assessment of power-electronics-based dc-distribution systems: Part 1: The root-locus technique," *Journal of Marine Engineering & Technology*, vol. 3, no. 2, pp. 13–21, 2004.